Life-Cycle of Structures and Infrastructure Systems – Biondini & Frangopol (Eds)

Preliminary assessment on the effects of longitudinal cracks on carbonation-induced corrosion

N. Russo, M. Gastaldi & F. Lollini
Department of Chemistry, Materials and Chemical Engineering "Giulio Natta", Politecnico di Milano, Milan, Italy

L. Schiavi & A. Strini
Construction Technologies Institute, National Research Council of Italy (ITC-CNR), San Giuliano Milanese, Milan, Italy

ABSTRACT: Currently available models for reinforced concrete (RC) durability still lack the inclusion of the effects of cracks, which are inevitable in concrete structures, and literature on the effects of cracks on carbonation-induced corrosion is scarce, especially in case of cracks longitudinal to the reinforcement. This paper presents some preliminary experimental results on the effects of longitudinal micro-cracks on carbonation-induced corrosion, initiation and propagation phases. Experimental tests were performed to evaluate the penetration of carbonation, under accelerated conditions, in cracked and uncracked concrete made with different cement types and *w/c* ratios. Corrosion propagation was monitored, through electrochemical techniques, in longitudinally cracked and uncracked RC specimens subjected either to natural or accelerated carbonation. Results showed a more marked effect of the micro-crack on carbonation penetration in more impervious concretes, while the presence of the micro-crack did not seem to significantly affect corrosion propagation, except when developing to rebar depth.

1 INTRODUCTION

Durability models, based on reliable modelling of the service life of reinforced concrete (RC) structures, are typically performed as a function of the initiation and propagation of corrosion of steel reinforcement, and are of fundamental importance to meet the sustainability targets in the construction field (Bertolini et al. 2013). However, even the most accredited models present some limitations that still need to be addressed to, such as the inclusion of the effects of cracks, which are inevitable in concrete and may alter the corrosive process. The limited knowledge concerning the effects of cracks on durability performances, especially in the case of carbonation-induced corrosion, contributed to slow their improvement at this regard.

Considering the penetration of carbonation in concrete, initially cracks lead to a general increase in the penetration rate of gaseous CO_2 from the environment. Subsequently, as carbonation proceeds, the precipitation of calcium carbonate in the form of calcite, vaterite and aragonite, that occupy a volume about 3 to 20% higher, leads to a partial closure of small cracks with time, as a form of carbonation-induced autogenous healing (Liu et al. 2021). Studies on carbonation penetration in unreinforced specimens and under accelerated carbonation showed that even micro-cracks (width at the exposed surface lower than 100 μm), could significantly affect the resistance to carbonation penetration. In Alahmad et al. (2009), a significant penetration of carbonation perpendicularly to crack walls was reported, similar to uncracked conditions for cracks wider than 60 μm, with a progressive decrease for cracks about 40 μm wide, and negligible for crack narrower than 9 μm. In Bogas et al. (2019), a method was proposed to retrieve the carbonation coefficient inside the crack, founding a carbonation coefficient 3.7 times higher in the crack with respect to uncracked concrete for a 100 μm wide artificial crack (obtained through metallic plates at fresh state), while in specimen with load-induced crack about 150 μm wide the increase resulted of

DOI: 10.1201/9781003323020-368

about 2.7 times. In Carević & Ignjatović (2019), some simulations were performed after carbonation depth measurements under accelerated conditions. It was estimated, according to *fib* Model Code 2010, that in the case of 300 μm wide crack, under natural carbonation, the service life of the structure would have been reduced of about three times with respect to uncracked conditions, assuming depassivation of steel as ultimate limit state.

Considering carbonation-induced corrosion in reinforced concrete, the presence of a crack can alter both the corrosion initiation and propagation processes. In fact, when a crack develops to rebar depth, an alteration in the protective alkaline environment normally provided by sound concrete may occur, and corrosion may preferentially take place where crack tip reaches the steel reinforcement (as observed for chloride-induced corrosion in Leporace-Guimil et al.). Moreover, once corrosion started, corrosion rate could further be increased by the generation of a small anode to large cathode ratio (ACI Committee 201, 2016). Literature on this topic is more limited in the case of cracks in the longitudinal direction of the reinforcement with respect to the transversal direction, which may form in bidimensional elements, or due to shrinkage, or plastic settlement of concrete. Longitudinal cracks may influence the corrosion process to a higher extent, since aggressive species (carbonation, moisture, oxygen, …) can more easily reach a wider area of embedded steel surface (Shaikh 2018). To conclude, the subject is not only complex due to the number of variables affecting durability parameters, but also to the different experimental procedures and materials used in different studies, which make it difficult to derive unambiguous conclusions.

This paper presents some preliminary experimental results on the effects of cracks on carbonation-induced corrosion initiation and propagation. Experimental tests were performed to evaluate the penetration of accelerated carbonation in cracked and uncracked unreinforced specimens, considering different cement types and w/c ratios, and cracked through a specifically developed loading procedure. Corrosion propagation was monitored in cracked and uncracked concrete specimens subjected either to natural or to accelerated carbonation. In this case, concrete was obtained with Portland-limestone cement and w/c of 0.45, reinforced with carbon steel bars, and cracked using the same procedure to obtain a longitudinal micro-crack. Electrochemical techniques were used to detect corrosion initiation in specimens subjected to natural carbonation (exposed to outdoor unsheltered environment), and to monitor corrosion propagation in specimens previously subjected to accelerated carbonation and then exposed to outdoor unsheltered environment, considering a different orientation for the cracked surface.

2 MATERIALS AND METHODS

2.1 *Specimens layout*

Unreinforced specimens were realized considering three different cement types, *i.e.* an ordinary Portland (OPC, type CEM I 42,5R according to EN 197-1), a Portland-Limestone (PLC, type CEM II/A-LL 42,5R), and a Pozzolanic cement (PC, type CEM IV/A(V) 42,5R-SR), and two *w/c* ratios, *i.e.* 0.45 and 0.55. Reinforced specimens were made only with PLC cement type and *w/c* of 0.45. The mixes with 0.45 *w/c* ratio were obtained considering 422 kg/m^3 of cement, 190 kg/m^3 of water and 1731 kg/m^3 of aggregates, while those with *w/c* ratio equal to 0.55 were obtained with 422 kg/m^3 of cement, 232 kg/m^3 of water and 1619 kg/m^3 of aggregates. All the aggregates were crushed calcareous type, subdivided into 5 grain size fractions, with maximum diameter of 9 mm. An acrylic-based superplasticizer was also added to the mixes with 0.45 of *w/c* ratio, to reach, at least, a S3 class of consistency. As reinforcement, carbon steel bars with 16 mm diameters were employed, subject to sandblasting and degreasing with acetone prior casting. Moreover, to avoid side effects, the two ends of each rebar were masked with a styrene-butadiene-modified cement mortar and epoxy, leaving a total length of 80 mm exposed to the concrete.

A total amount of 6 unreinforced specimens per each cement type and *w/c* ratio were realized, out of which 2 in uncracked and 4 in cracked configuration, while a total amount of 16 reinforced specimens were realized, out of which 4 in sound (S), 9 in cracked (C) and 3 in heavily cracked (HC) configuration. All the specimens were characterized by prismatic geometry, with dimensions 120×90×50 mm, as reported in Figure 1. In cracked configuration, specimens presented

a longitudinal notch, about 3 mm depth, to promote the formation of the crack during the cracking procedure. In reinforced configuration, specimens were equipped with one carbon steel rebar (concrete cover thickness of 15 mm), an activated titanium wire (reference electrode) and a titanium wire (counter-electrode) for electrochemical measurements. Both unreinforced and reinforced cracked specimens were subjected to a specifically developed cracking procedure, within 24 hours after casting (thus to have a lower concrete mechanical resistance and a less brittle behaviour). The method was a sort of three-point bending procedure to induce a longitudinal micro-crack in correspondence of the notch. Specimens were encased in a steel confinement system and placed in a universal testing machine with the notch facing downwards, and interposing three stripes of synthetic elastomer membrane, 1.2 mm thick. Two were placed along the downward corners of the specimen, as the supports, and the other in central position on the upward face, as the loading pin. A displacement-controlled load was then applied, equal to 0.5 mm/min in the vertical direction. In unreinforced configuration, the load was applied until an overload level 45-55% higher than that corresponding to the first appearance of the crack was reached. Cracks were measured at the end of exposure to carbonation with the same procedure as in Russo et al. 2020, and resulted 30-160 μm wide and 30-40 mm deep. In reinforced configuration, the load was applied until the simultaneous appearance of the crack on both sides of the specimen, at least one of which was up to the rebar. To the 3 more heavily cracked specimens a further overload of 10 % was applied. For further details on the procedure and on the obtained cracks see past publications (Russo et al. 2020, Russo et al., in press). After the cracking procedure specimens were kept, together with the uncracked ones, in a curing chamber at a temperature of 20 °C and relative humidity higher than 90%, until the starting of tests.

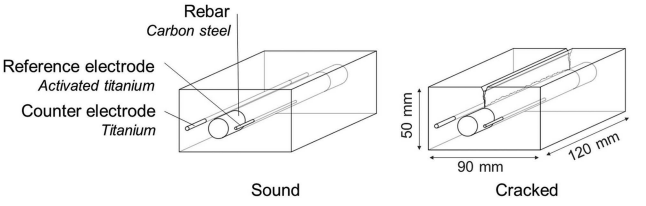

Figure 1. Schematic representation of sound and cracked concrete specimens in reinforced configuration.

2.2 *Resistance to penetration of carbonation*

Specimens were moist cured for 28 days and subsequently were pre-conditioned and prepared for accelerated carbonation test according to EN 12390-12. All the surfaces of each specimen were then sealed with epoxy, except for the cast surface to be exposed to carbonation. Accelerated carbonation was performed in a chamber with 3% of CO_2 concentration, 60% of relative humidity and 20 °C of temperature for 30 and 70 days of exposure. At each exposure time, one portion of the specimen was split and phenolphthalein was sprayed, in order to highlight the carbonation profile. The split surface of the remaining part of the specimen was sealed again to be exposed for the other exposure time. Carbonation depth measurements were measured with a calliper, and were taken in correspondence of the central point and on three other points on each side, spaced 10 mm each (7 points in total). In cracked configuration the central measurement, *i.e.* in correspondence of the crack, was taken in correspondence of the maximum penetration depth, excluding the notch. The accelerated carbonation coefficient, K_{AC}, was derived according to the formula:

$$x = K_{AC} \cdot \sqrt{t} \tag{1}$$

where x = average carbonation depth; t = time. At each exposure time, in sound configuration a single coefficient was evaluated (K_s), considering the average penetration depth. In cracked configuration two coefficients were evaluated, one in correspondence of the crack (K_{cr}), considering the maximum penetration depth, and the other in the uncracked part of the specimen (K_{uncr}), considering measurements points at ±20 and ±30 mm from the central crack.

2.3 *Carbonation-induced corrosion monitoring*

Reinforced specimens for the monitoring of corrosion were moist-cured for 7 days. After curing, three cracked specimens were exposed to outdoor unsheltered conditions, one with the surface containing the crack oriented horizontally, one vertically and one heavily cracked horizontally. Specimens were periodically monitored, thorough electrochemical measurements, to detect corrosion initiation and monitor corrosion propagation. The other reinforced specimens in uncracked and cracked configurations were exposed to accelerated carbonation to induce corrosion initiation, in the carbonation chamber with 3% of CO_2 concentration, 60% of relative humidity and 20 °C of temperature. Specimens were periodically taken out of the carbonation chamber to electrochemically assess whether corrosion was initiated. After corrosion initiation was detected, specimens were exposed to external unsheltered conditions, considering either horizontal orientation or vertical orientation of the crack (as in a floor or a vertical element, respectively).

As electrochemical measurements, the half-cell potential (E_{corr}) was measured versus a saturated calomel electrode (SCE), placing the electrode on the specimen surface in correspondence of the central part of the rebar, while corrosion current density (i_{corr}) was measured through linear polarization resistance measurement (R_p) according to the equation:

$$i_{corr} = \frac{B}{R_p \cdot A} \tag{2}$$

where A = surface of rebar exposed to concrete; B = assumed equal to 26 mV.

3 RESULTS AND DISCUSSION

3.1 *Effects of micro-cracks on penetration of carbonation*

Figure 2 reports the results obtained in terms of K_{AC}, for the different exposure times and for the different concrete types, where histograms represent average values and error bars represent maximum and minimum values. In the Figure, the different mixes are identified with a label recalling the cement type (OPC for Ordinary Portland, PLC for Portland-limestone and PC for Pozzolanic cement type) followed by the *w/c* ratio. Considering sound and uncracked configurations, a quite good reproducibility of results was obtained in replicate specimens, and, moreover, for each concrete type K_{AC} was very similar for the two configurations. Similar results were also obtained considering the same mix at different exposure times. This result was expected, since carbonation in concrete is generally believed to be not affected by an ageing factor, unlike chloride penetration. To discuss the effect of cement type and *w/c* ratio, a single value of K_{AC} can be therefore considered, by averaging the values at both the exposure times in sound and uncracked conditions (Table 1).

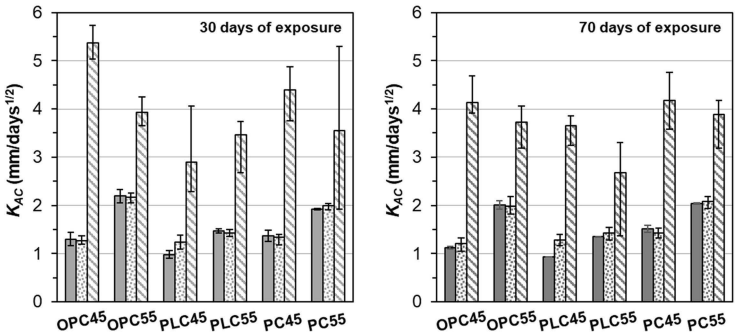

Figure 2. Average accelerated carbonation coefficient (KAC) and variability in sound (Ks, solid), uncracked (Kuncr, dotted) and cracked (Kcr, hatched) configurations, for different concrete types, after 30 (left) and 70 (right) days of exposure.

Concretes made with *w/c* equal to 0.45 showed similar K_{AC} in sound and uncracked conditions, except PLC45, for which the sound value unexpectedly resulted lower than 1 mm/days$^{1/2}$. If for this cement type the value in uncracked condition is considered more accurate, the carbonation coefficient for different cement types resulted quite similar, between 1.2 and 1.4 mm/days$^{1/2}$. As expected, higher K_{AC} were found for concretes with *w/c* of 0.55, since these concretes were characterized by higher permeability, which is considered to be one of the main factors affecting the diffusion of carbon dioxide in concrete (Bertolini et al. 2013). K_{AC} for these concretes resulted included between 1.2 and 2 mm/days$^{1/2}$, showing a percentage increment that depended on the cement type, *i.e* about 40% for PC, 30% for OPC, and 15% for PLC.

Table 1. Average K_{AC} evaluated considering both the exposure times.

	OPC45	OPC55	PLC45	PLC55	PC45	PC55
K_s *(mm/days$^{1/2}$)*	1.21	2.10	0.96	1.42	1.44	1.98
K_{uncr} *(mm/days$^{1/2}$)*	1.24	2.07	1.26	1.43	1.38	2.03

Considering the effect of micro-cracks, these always led to a significant increase in the carbonation depth and therefore in the carbonation coefficient, and in the scatter of data among replicate specimens and for the same concrete type at different exposure duration (hatched histograms and error bars in Figure 2). It is worth noting, however, that this high scatter is also related to the fact that results at different exposure times were obtained on different specimens, characterized by different crack parameters, as well as replicate specimens for the same exposure duration may have been characterized by variable crack widths and depths. Moreover, the adopted cracking procedure did not prove to guarantee replicable cracks widths and depths (Russo et al. 2020). For this reason, the results at different exposure times were not averaged to find a single K_{AC}. To discuss the effects of the micro-crack on the carbonation coefficient, Figure 3 shows the ratio between K_{AC} in micro-cracked and uncracked condition (K_{cr}/K_{uncr}), as a function of K_{uncr}.

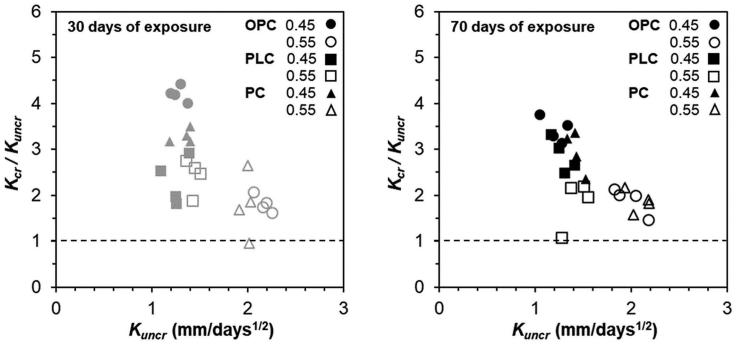

Figure 3. Increase in accelerated carbonation coefficient in the crack with respect to uncracked conditions (K_{cr}/K_{uncr}) as a function of accelerated carbonation coefficient in uncracked conditions, for different concrete types and after 30 (left) and 70 (right) days of exposure.

As can be noticed in Figure 3 an increase in the carbonation coefficient in the micro-crack always occurred, at both the exposure times. Moreover, an increasing trend in the ratio K_{cr}/K_{uncr} could be detected, for decreasing values of K_{uncr} (less permeable concretes). This effect was more pronounced for concretes with *w/c* of 0.45 (filled symbols), showing K_{cr}/K_{uncr} between 2 and 4.5, considering both the exposure times, and less pronounced for concretes with *w/c* of 0.55 (empty symbols), being K_{cr}/K_{uncr} mostly between 1 and 2.5. Similar results were obtained by the writing Authors with regard to chloride penetration resistance (Russo et al. 2020, Russo et al. 2022), confirming that a more marked effect of the micro-crack on concrete durability may occur for more impervious concretes. However, the presence of micro-cracks may not be of high concern for

concretes characterized by the *w/c* ratios typically used for structures subject to carbonation-induced corrosion, which according to EN 206 are 0.50 for exposure class XC4 and 0.55 for XC3.

3.2 *Effects of micro-cracks on corrosion initiation and propagation*

Figure 4 shows the electrochemical monitoring of corrosion potential (E_{corr}) and corrosion current density (i_{corr}), for cracked and highly cracked specimens exposed to outdoor unsheltered conditions. In particular, one cracked specimen was exposed with the crack in horizontal direction (CH), another one in vertical (CV), while one highly cracked in horizontal direction (HCH). The Figure reports also the outdoor climatic conditions, *i.e.* the daily cumulative rain and the daily average temperature (dark and light grey lines respectively). It can be noticed that over almost two years of exposure temperature fluctuated between 0°C and 30°C, while rain was in general quite scarce, with only 56 days with more than 5 mm of cumulative rain recorded. During the first half of exposure period (up to about 200 days of exposure), and especially in correspondence of the more wet days, HCH specimen already showed significantly lower values of E_{corr} (−200 ÷ −250 mV vs SCE) associated to i_{corr} values around 2 mA/m^2. It is reasonable to assume that in this specimen the crack developed to rebar depth, by analogy with some specimens realized and cracked with the same procedure but exposed to chlorides (Russo et al., in press), which may have led to corrosion initiation within the first 200 days of exposure. Subsequently, however, during the second half of the exposure period, E_{corr} was on average increased, and i_{corr} remained at values around 1 mA/m^2 or even lower. This may be associated to a drier climate during this period, or, eventually, to a partial or total closure of the crack due to self-healing and re-passivation of steel rebar. Further monitoring as well as destructive tests are needed to further investigate this aspect.

No significant difference in electrochemical behaviour was instead detected between the two cracked specimens with differently oriented cracked surface (CH and CV), whose values of i_{corr} always remained around 1 mA/m^2 or even lower, suggesting rebar passivity. For these two specimens it is reasonable to assume that the crack (and carbonation) did not reach rebar depth or, at least, did not involve a sufficiently wide area of steel to detect corrosion initiation with linear polarization method.

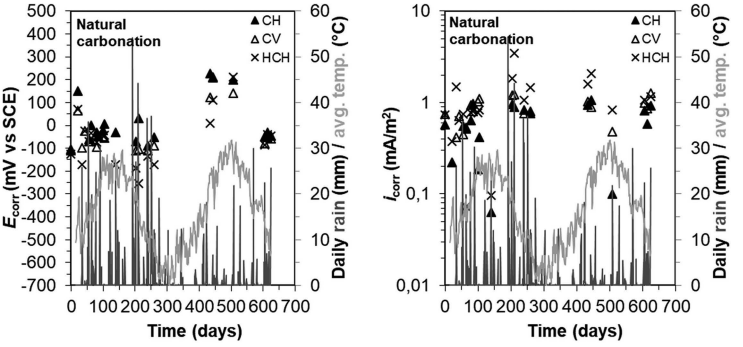

Figure 4. Trend in time of corrosion potential (left) and corrosion current density (right) for reinforced cracked (C) and highly cracked (HC) specimens subjected to natural carbonation with horizontal (H) or vertical (V) orientation.

Figure 5 shows the electrochemical monitoring for sound (S), cracked (C) and highly cracked (HC) specimens subjected to accelerated carbonation to induce corrosion initiation and external outdoor exposure to monitor natural corrosion propagation, with different crack orientation. In the Figure, the hatched area highlights the period in which specimens were in the carbonation chamber, the solid blue and grey areas highlight the measurements that were taken after 4 days of exposure to partial immersion and after one week in the curing chamber (T=20°C, RH>90%), respectively. These measurements were performed to verify, at two different humidity

contents, the corrosion initiation. Subsequently, the dark and light grey lines report the trend of the daily cumulative rain and the daily average temperature during external outdoor exposure.

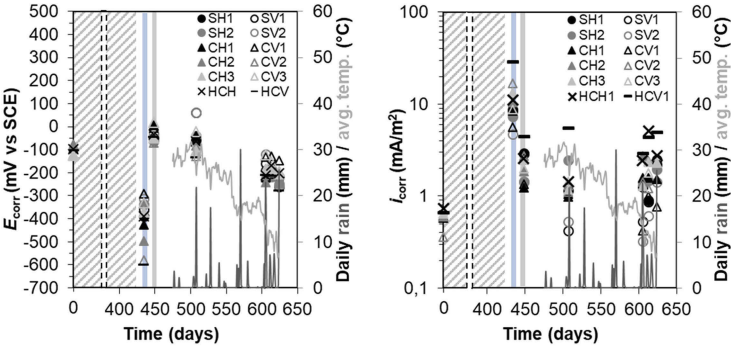

Figure 5. Trend in time of corrosion potential (left) and corrosion current density (right) for reinforced sound (S), cracked (C) and highly cracked (HC) specimens subjected to accelerated carbonation and natural corrosion propagation at outdoor exposure with horizontal (H) or vertical (V) orientation.

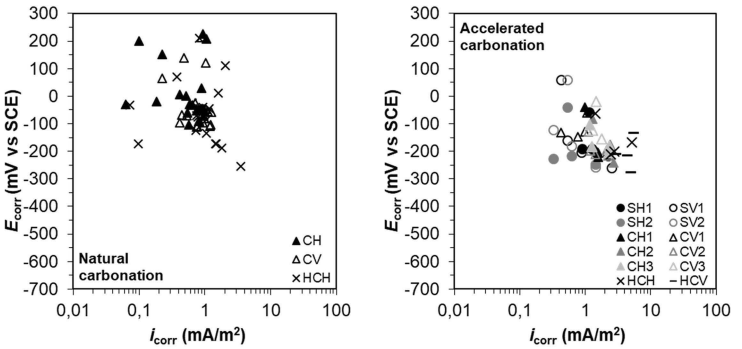

Figure 6. Corrosion potential as a function of corrosion current density for specimens subjected to natural (left) and accelerated (right) carbonation, in sound (S), cracked (C) and highly cracked (HC) configurations, with horizontal (H) or vertical (V) orientation.

The lowest E_{corr} values (−300 ÷ −600 mV vs SCE), together with the highest i_{corr} values (up to 9 mA/m^2 for sound, S, 17 mA/m^2 for cracked, C, and 29 mA/m^2 for highly cracked concrete, HC), were detected as soon after the end of exposure to the carbonation chamber, at partial immersion conditions, confirming that carbonation arrived at rebar depth causing corrosion initiation in all the configurations. At curing chamber conditions, a neat increase of E_{corr} was detected (0 ÷ −100 mV vs SCE), while i_{corr} decreased of roughly one order of magnitude (1 ÷ 5 mA/m^2), due to a lower moisture content in concrete and therefore higher concrete electrical resistivity. Specimens were then moved at external conditions during summer and fall, characterized by mild temperatures (15 ÷ 30°C) and very low cumulative rain. Due to the prolonged drought, the values of E_{corr} and i_{corr} remained stable, at values close to the curing chamber conditions, without any particular difference between the cracked (C) and sound (S) conditions and vertical or horizontal orientation, unless for the two sound specimens exposed with vertical orientation, that showed particularly low i_{corr} (0.5 mA/m^2). The latest measurements were performed during winter, characterized by a higher amount of precipitations, but no particular difference in values of E_{corr} and i_{corr} were detected, even though i_{corr} seems to slightly increase in time. Again, specimens characterized by vertical orientation (hollow symbols) seemed on average to be characterized by lower values of $i_{corr,}$ while highly cracked specimens by higher i_{corr}, independently from crack orientation.

The same conclusions can be drawn if considering E_{corr} as a function of i_{corr} (Figure 6), where all the measurements during corrosion monitoring are reported for specimens subjected to natural carbonation, while only measurements during corrosion propagation at external exposure are reported for specimens previously subjected to accelerated carbonation. These results may imply that if a crack develops to rebar depth, not only corrosion initiation time may be reduced (excluding possible self-healing effects, not proved to the writing time), but also the corrosion propagation stage, due to a higher corrosion rate. On the other hand, comparable propagation of corrosion may be assumed in carbonated concrete if the crack does not develop to rebar depth, due to comparable corrosion rate values.

4 CONCLUSIONS

This study reports some preliminary results on the effects of cracks on carbonation-induced corrosion. Penetration of carbonation was tested under accelerated exposure conditions in cracked and uncracked unreinforced specimens, while corrosion propagation was monitored in cracked and uncracked concrete specimens subjected either to natural or to accelerated carbonation, considering different orientations of the cracked surface. The adopted cracking procedure was kept constant, to induce micro-cracks in direction longitudinal to the specimen (and the rebar). Carbonation penetration was evaluated through a colorimetric technique while corrosion was monitored through electrochemical techniques to measure corrosion potential and current density.

Results showed that for cracks 30-160 μm wide and 30-40 mm deep, a more marked effect of the crack on carbonation penetration may occur in more impervious concretes, leading to an increase in the carbonation coefficient up to 4 times. The presence of a crack developing down to rebar depth led corrosion initiation within the first 200 days of exposure, and to higher corrosion rates during corrosion propagation. In specimens where crack was supposed not to develop to rebar depth, no particular effect of the presence of the crack, nor of its orientation, was detected.

REFERENCES

ACI Committee 201 2016. *ACI 201.2R-16 Guide to Durable Concrete*. American Concrete Institute.

Alahmad, S., Toumi, A., Verdier J. & François, R. 2009. Effect of crack opening on carbon dioxide penetration in cracked mortar samples. *Materials and Structures* 42(5): 559–566.

Bertolini, L., Elsener, B., Pedeferri, P. Redaelli E. & Polder, R.B. 2013. *Corrosion of Steel in Concrete: Prevention, Diagnosis, Repair, Second Edition*. Weinheim: Wiley-VCH.

Bogas, J.A., Carriço A. & Pontes, J. 2019. Influence of cracking on the capillary absorption and carbonation of structural lightweight aggregate concrete. *Cement and Concrete Composites* 104, 103382.

Carević, V. & Ignjatović, I. 2019. Influence of loading cracks on the carbonation resistance of RC elements. *Construction and Building Materials* 227, 116583.

Leporace-Guimil, B., Russo, N., Lollini, F. & Conforti, A. 2023. Morphological and mechanical characterization of reinforcement in cracked elements exposed to chloride-induced corrosion. *Construction and Building Materials* 364, 129822.

Liu, Z., Van den Heede P. & De Belie, N. 2021. Effect of the mechanical load on the carbonation of concrete: A review of the underlying mechanisms, test methods, and results. *Materials* 14(16), 4407.

Shaikh, F. 2018. Effect of Cracking on Corrosion of Steel in Concrete. *International Journal of Concrete Structures and Materials* 12(1), 3.

Russo, N., Gastaldi, M., Marras, P., Schiavi, L., Strini, A., & Lollini, F. 2020. Effects of load-induced micro-cracks on chloride penetration resistance in different types of concrete. *Materials and Structures* 53(6): 1–14.

Russo, N., Gastaldi, M., Schiavi, L., Strini, A., & Lollini, F. 2022. Chloride penetration resistance in sound and micro-cracked concretes through different experimental techniques. *Construction and Building Materials* 343, 128098.

Russo, N., Gastaldi, M., Schiavi, L., Strini, A., & Lollini, F. 2023. Effects of cracks on chloride-induced corrosion initiation and propagation of carbon and stainless steel rebar. *Structural Concrete* 24(1):156–169.